Journal of Guidance, Control, and Dynamics
Vol. 41, No. 6, June 2018

Engineering Notes

Fully Coupled Reaction Wheel Static and Dynamic Imbalance for Spacecraft Jitter Modeling

John Alcorn,* Cody Allard,* and Hanspeter Schaub†
University of Colorado, Boulder, Colorado 80309-0431

DOI: 10.2514/1.G003277

Nomenclature

B_c, W_{c_i}	=	rigid-hub center of mass location, ith wheel-frame center of mass location
$\{\hat{\boldsymbol{b}}_1, \hat{\boldsymbol{b}}_2, \hat{\boldsymbol{b}}_3\}$	=	body-frame basis vectors
$\boldsymbol{c}$	=	vector from point B to center of mass of the spacecraft C, cm
d_i	=	center of mass offset of ith reaction wheel, mm
$\{\hat{\boldsymbol{g}}_{s_i}, \hat{\boldsymbol{w}}_{2_i}, \hat{\boldsymbol{w}}_{3_i}\}$	=	ith wheel-frame basis vectors
$\boldsymbol{H}_{\mathrm{sc},B}$	=	angular momentum vector of spacecraft about point B, N · m · s
$[I_{\mathrm{hub},B_c}]$	=	inertia tensor of rigid-hub about point B_c, kg · m^2
$[I_{\mathrm{rw}_i,W_{c_i}}]$	=	inertia tensor of ith reaction wheel about point W_{c_i}, kg · m^2
$[I_{\mathrm{sc},B}]$	=	inertia tensor of spacecraft about point B, kg · m^2
m_{sc}, m_{hub}, m_{rw_i}	=	mass of spacecraft, hub, and ith reaction wheel, respectively
N, B, W_i	=	inertial-frame origin, body-frame origin, ith wheel-frame origin
$\mathcal{N}$, $\mathcal{B}$, $\mathcal{M}_i$, $\mathcal{W}_i$	=	reference frame of inertial, body, ith motor, and ith wheel, respectively
$\boldsymbol{r}_{B/N}$	=	position vector of B with respect to N, m
$\dot{\boldsymbol{r}}_{B/N}$	=	inertial velocity vector of B with respect to N, m/s
U_{d_i}	=	dynamic imbalance parameter, g · cm^2
U_{s_i}	=	static imbalance parameter, g · cm
u_{s_i}	=	reaction wheel motor torque, mN · m
$\dot{\boldsymbol{v}}$	=	time derivative of a vector $\boldsymbol{v}$ with respect to the inertial frame $\mathcal{N}$
$\boldsymbol{v}'$	=	time derivative of a vector $\boldsymbol{v}$ with respect to the body frame $\mathcal{B}$
θ_i	=	ith wheel angle, deg
$\boldsymbol{\omega}_{\mathcal{B}/\mathcal{N}}$	=	inertial angular velocity vector of $\mathcal{B}$ frame with respect to $\mathcal{N}$ frame, deg/s
$\boldsymbol{\sigma}_{\mathcal{B}/\mathcal{N}}$	=	modified Rodrigues parameters representing $\mathcal{B}$ frame with respect to $\mathcal{N}$ frame
Ω_i	=	ith wheel speed relative to the body frame, RPM

I. Introduction

Momentum exchange devices are a fundamental component of most spacecraft for both coarse attitude control and precision pointing. Many modern spacecraft include three or more reaction wheels (RWs), which consist of a flywheel attached to a motor and bearing fixed to the spacecraft. A challenge to using RWs is that they may induce jitter due to mass imbalances in the RW. Characterization and mitigation of RW-induced jitter on a spacecraft is important to many missions due to the increasingly rigorous attitude stability requirements and the necessity of avoiding excitation of the spacecraft's structural modes. Excessive vibration of a spacecraft may be detrimental to its instruments and operation. Additionally, many instruments require the spacecraft to be held extremely steady in order to effectively operate or collect data. Optical instruments in particular often require attitude stability of less than 1 arc-second per second in order to avoid optical smear or similar effects [1,2]. Vibration isolation has long been a method of dulling the effects of wheel jitter [3]. Various methods of vibration isolation have been proposed, including magnetic suspension of RWs as a means of circumventing the jitter problem [4,5].

RW-induced vibration on a spacecraft is usually characterized through experimentation before flight in order to validate requirements. Empirical models of RWs allow static and dynamic imbalance parameters to be extracted [6,7]. In addition to experimental demonstration of RW performance on an integrated spacecraft, it is of interest to use an analytic model of an RW for simulation in the early stages of spacecraft development. A popular simplified model of RW jitter involves including forces and torques resulting from RW static and dynamic imbalances as external disturbances [3,8,9]. Static imbalance is when the center of mass of the RW is not coincident with the spin axis, and dynamic imbalance is due to off-diagonal inertia matrix terms with respect to the spin axis frame. This model is well established and attractive due to its low computational requirements—force and torque of jitter are simply proportional to wheel speed squared. Furthermore, the simplified formulation allows a model to be constructed directly from the typical RW manufacturer imbalance specifications: static imbalance and dynamic imbalance. This allows RW mass imbalances to be implemented as lumped parameters instead of using specific terms such as RW center of mass location and inertia tensor [3]. Previous literature puts emphasis on empirical modeling of RW jitter and the effects of RW jitter within context of spacecraft flexible dynamics [10–12].

Regarding modeling the momentum exchange device jitter with a first-principles approach, Zhang and Zhang discuss a fully coupled model of control moment gyro (CMG) imbalance [13]. While this contains gyro frame imbalance modeling not required for RWs, the results are presented without a full derivation and the paper does not provide the complete system equations of motion (EOMs). These partial imbalanced momentum exchange device results also do not discuss how to tie typical manufacturers' imbalance specifications directly to the imbalance parameter modeling. Reference [5] develops the spacecraft EOMs with magnetically suspended RWs, where the RW center of mass moves relative to the body. However, this magnetic levitation introduces additional degrees of freedom (DOFs) and modeling challenges not present in a body-locked imbalanced RW as studied in this paper.

Presented as Paper 2016-5686 at the AIAA/AAS Astrodynamics Specialist Conference, Long Beach, CA, 12–15 September 2016; received 19 August 2017; revision received 5 December 2017; accepted for publication 6 December 2017; published online 23 January 2018.

*Graduate Research Assistant, Department of Aerospace Engineering Sciences, 431 UCB, Colorado Center for Astrodynamics Research. Student Member AIAA.

†Alfred T. and Betty E. Look Professor of Engineering, Department of Aerospace Engineering Sciences, 431 UCB, Colorado Center for Astrodynamics Research. Associate Fellow AIAA.

The simplified model for representing RW jitter due to static and dynamic imbalances is not physically realistic due to the nonconservative nature of adding a system-internal forcing effect as an external disturbance [14]. The resulting model considers only the impact of the wheel onto the spacecraft but neglects how the spacecraft impacts the wheel motion. The resulting one-way coupled simplified model has the primary benefits of algebraic simplicity of the jitter equations and the associated fast computational evaluation. For spacecraft dynamics analysis purposes the nonphysical nature of the simplified model does not necessarily present a problem if the RWs are well balanced with respect to the overall size of the spacecraft. However, depending on the quality of the RW balance in relation to the spacecraft size this approach may become problematic. Furthermore, the simplified model does not allow for energy and momentum code validation checks. When verifying the computer simulation code the spacecraft energy and momentum checks are critical tools of the dynamics validation process. Even for a spacecraft simulation that only includes RW jitter, complete verification of the model is difficult because without energy and momentum checks a truth model is difficult to create. If the model of the spacecraft has other complex behaviors such as solar panel flexing or fuel slosh, the importance of energy and momentum checks increases rapidly. The coupled nature of these complex spacecraft systems results in severe challenges with debugging and verification. The energy and momentum checks become essential in this process.

This paper presents a first-principles–based derivation of the EOMs for a spacecraft with N_{rw} RWs subject to general static and dynamic imbalances. The resulting formulation retains the true physics governing this fully coupled jitter phenomenon. As a result, energy and momentum checks are available using this model. A Newtonian/Eulerian formulation approach is employed. Because the primary spacecraft body, called the hub, is considered to be rigid, flexible dynamics are not considered in this paper. However, the formulation is developed in such a way that adding other modes such as flexing and fuel slosh is relatively simple [15,16]. Additionally, the relationship between the first-principles–based fully coupled RW model and the manufacturers' specifications characterizing RW static and dynamic imbalances is discussed. This is of interest as the manufacturers provide their basic first-order RW jitter performance using the static and dynamic imbalance parameters. Numerical simulations investigate the validity of the presented RW EOMs solution by studying the system energy and angular momentum responses.

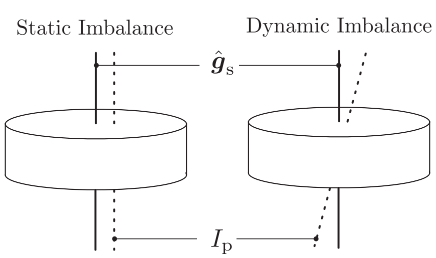

Fig. 1 Reaction wheel static and dynamic imbalance.

II. Problem Statement

An offset in the center of mass of the RW from the spin axis, denoted static imbalance, results in an internal force and torque on the spacecraft. An asymmetric distribution of mass about the RW spin axis is denoted as the dynamic imbalance and produces an internal disturbance torque onto the spacecraft. Figure 1 explains these imbalances geometrically. I_p is a line that is coincident with the center mass of the RW and illustrates a principal axis of the RW. The static imbalance results in a center of mass offset of the RW but does not change the direction of the principal axes. The dynamic imbalance is a result of one of the principal axes not being aligned with the spin axis. Deflection of the RW wheel bearing due to static and dynamic imbalances further affects the vibrational modes of the system; however, this effect is beyond the scope of this work and is not being considered. This paper investigates modeling these classical static and dynamic imbalance behaviors in a first-principles–based approach. With this jitter model the RW is still treated as a rigid component with a body-fixed rotation axis, but the rotation axis is not necessarily aligned with one of the RW principal axes, and the RW center of mass is off-set from this rotation axis by a distance d_i.

When deriving the EOMs for a spacecraft with N_{rw} RWs, an important assumption is made in that the RWs are symmetric and results in the EOMs to be simplified to a convenient and compact form [14]. However, if the RWs are imbalanced the EOMs have to be re-derived to account for the fully coupled dynamics between the RWs and the spacecraft. This paper follows a development path using Newtonian and Eulerian mechanics using a formulation that uses a minimal coordinate description [14].

Figure 2 shows the frame and variable definitions used for this problem. The formulation involves a rigid-hub with its center of mass location labeled as point B_c, and N_{rw} RWs with their center of mass locations labeled as W_{c_i}. The frames being used for this formulation are the body-fixed frame, $\mathcal{B}$: $\{\hat{\boldsymbol{b}}_1, \hat{\boldsymbol{b}}_2, \hat{\boldsymbol{b}}_3\}$; the motor frame of the ith RW, $\mathcal{M}_i$: $\{\hat{\boldsymbol{m}}_{s_i}, \hat{\boldsymbol{m}}_{2_i}, \hat{\boldsymbol{m}}_{3_i}\}$, which is also body-fixed; and the wheel-fixed frame of the ith RW, $\mathcal{W}_i$: $\{\hat{\boldsymbol{g}}_{s_i}, \hat{\boldsymbol{w}}_{2_i}, \hat{\boldsymbol{w}}_{3_i}\}$. The dynamics are modeled with respect to the $\mathcal{B}$ frame, which can be generally oriented. The $\mathcal{W}_i$ frame is oriented such that the $\hat{\boldsymbol{g}}_{s_i}$ axis is aligned with the RW spin axis, which is the same as the motor torque axis $\hat{\boldsymbol{m}}_{s_i}$; the $\hat{\boldsymbol{w}}_{2_i}$ axis is perpendicular to $\hat{\boldsymbol{g}}_{s_i}$ and points in the direction toward the RW center of mass W_{c_i}. The $\hat{\boldsymbol{w}}_{3_i}$ completes the right-hand rule. The $\mathcal{M}_i$ frame is defined as being equal to the $\mathcal{W}_i$ frame at the beginning of the simulation, and therefore the $\mathcal{W}_i$ and $\mathcal{M}_i$ frames are offset by an angle, θ_i, about the $\hat{\boldsymbol{m}}_{s_i} = \hat{\boldsymbol{g}}_{s_i}$ axes.

A few more key variables in Fig. 2 need to be defined. The rigid spacecraft structure without the RWs is called the hub. Point B is the origin of the $\mathcal{B}$ frame and is a general body-fixed point that does not

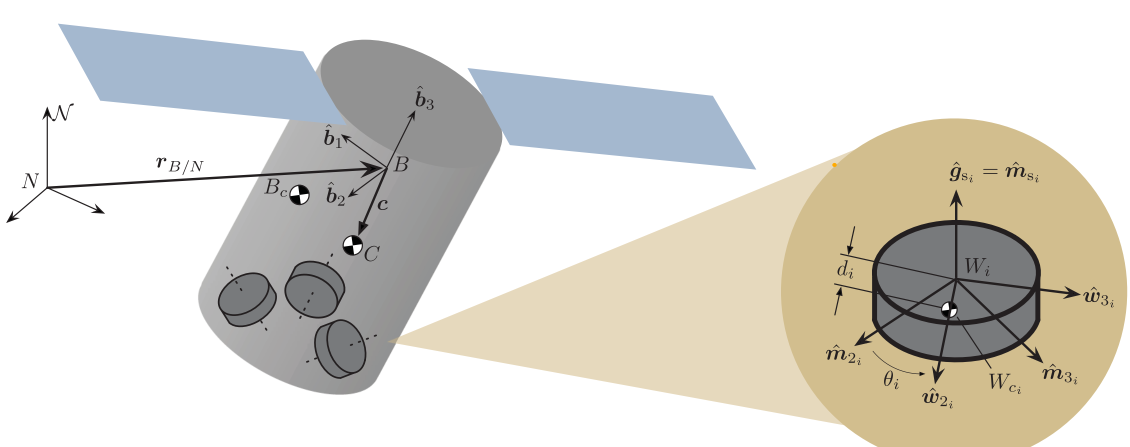

Fig. 2 Reference frame and variable definitions.

have to be identical to the total spacecraft center of mass or the rigid-hub center of mass B_c. Point W_i is the origin of the $\mathcal{W}_i$ frame and can also have any location relative to point B. Point C is the center of mass of the total spacecraft system including the rigid-hub and the RWs. Because of the RW imbalance, the vector $\boldsymbol{c}$, which points from point B to point C, will vary as seen by a body-fixed observer. The scalar variable d_i is the center of mass offset of the RW, or the distance from the spin axis, $\hat{\boldsymbol{g}}_{s_i}$ to W_{c_i}. Finally, the inertial frame orientation is defined through $\mathcal{N}$: $\{\hat{\boldsymbol{n}}_1, \hat{\boldsymbol{n}}_2, \hat{\boldsymbol{n}}_3\}$, and the origin of the inertial frame is labeled as N.

III. Equations of Motion

The system under consideration is an $N_{\text{rw}} + 6$ DOF system with the following second-order terms: inertial translational acceleration of point B with respect to point N $\ddot{\boldsymbol{r}}_{B/N}$, spacecraft rotational inertial angular acceleration $\dot{\boldsymbol{\omega}}_{\mathcal{B}/\mathcal{N}}$, and the angular acceleration of each RW $\dot{\Omega}_1, \ldots, \dot{\Omega}_{N_{\text{rw}}}$ relative to the spacecraft hub. Thus, a total of $N_{\text{rw}} + 6$ equations must be developed in order to solve for all second-order terms. Section III.A describes the derivation of the translational EOM and represents 3 DOFs, Sec. III.B describes the rotational motion and represents 3 DOFs, and Sec. III.C describes the motor torque equation and represents N_{rw} DOFs.

A. Translational Motion

For the dynamical system considered, the center of mass of the spacecraft is not constant with respect to the body frame. This results in the necessity to track the center of mass of the spacecraft and its corresponding acceleration. Following a similar derivation as seen in [15], the derivation begins with Newton's second law for the center of mass of the spacecraft seen in Eq. (1).

$$\ddot{\boldsymbol{r}}_{C/N} = \frac{\boldsymbol{F}}{m_{\text{sc}}} \tag{1}$$

Here $\boldsymbol{F}$ is the sum of the external forces on the spacecraft, which has a mass labeled as m_{sc}. The vector and inertia tensor notation being used for this work can be seen in [14]. For example, the vector $\boldsymbol{v}_{B/A}$ is a vector that points from point A to B. The time derivative of a vector $\boldsymbol{v}$ as seen by an inertial frame $\mathcal{N}$ is denoted by ${}^{\mathcal{N}}\mathrm{d}\boldsymbol{v}/\mathrm{d}t \equiv \dot{\boldsymbol{v}}$, whereas the time derivative with respect to a spacecraft body-fixed frame $\mathcal{B}$ is denoted by ${}^{\mathcal{B}}\mathrm{d}\boldsymbol{v}/\mathrm{d}t \equiv \boldsymbol{v}'$.

Ultimately the acceleration of the body-frame or point B is desired, which is expressed through

$$\ddot{\boldsymbol{r}}_{B/N} = \ddot{\boldsymbol{r}}_{C/N} - \ddot{\boldsymbol{c}} \tag{2}$$

where the center of mass position vector relative to B is defined as

$$\boldsymbol{c} = \frac{1}{m_{\text{sc}}}\left(m_{\text{hub}}\boldsymbol{r}_{B_c/B} + \sum_{i=1}^{N_{\text{rw}}} m_{\text{rw}_i}\boldsymbol{r}_{W_{c_i}/B}\right) \tag{3}$$

Taking the first and second body-relative time derivatives of point $\boldsymbol{c}$ results in

$$\boldsymbol{c}' = \frac{1}{m_{\text{sc}}}\sum_{i=1}^{N_{\text{rw}}} m_{\text{rw}_i}\boldsymbol{r}'_{W_{c_i}/B} \qquad \boldsymbol{c}'' = \frac{1}{m_{\text{sc}}}\sum_{i=1}^{N_{\text{rw}}} m_{\text{rw}_i}\boldsymbol{r}''_{W_{c_i}/B} \tag{4}$$

because $\boldsymbol{r}_{B_c/B}$ is a body-fixed vector. The ith RW wheel center of mass location relative to B is given by $\boldsymbol{r}_{W_{c_i}/B}$.

$$\boldsymbol{r}_{W_{c_i}/B} = \boldsymbol{r}_{W_i/B} + \boldsymbol{r}_{W_{c_i}/W_i} = \boldsymbol{r}_{W_i/B} + d_i\hat{\boldsymbol{w}}_{2_i} \tag{5}$$

The first and second body-relative time derivatives of $\boldsymbol{r}_{W_{c_i}/B}$ yield

$$\boxed{\boldsymbol{r}'_{W_{c_i}/B} = d\hat{\boldsymbol{w}}'_{2_i} = \boldsymbol{\omega}_{\mathcal{W}_i/\mathcal{B}} \times d_i\boldsymbol{w}_{2_i} = \Omega_i\hat{\boldsymbol{g}}_{s_i} \times d_i\boldsymbol{w}_{2_i} = d_i\Omega_i\hat{\boldsymbol{w}}_{3_i}} \tag{6}$$

$$\boldsymbol{r}''_{W_{c_i}/B} = \Omega_i\hat{\boldsymbol{g}}_{s_i} \times d_i\Omega_i\hat{\boldsymbol{w}}_{3_i} = d_i\dot{\Omega}_i\hat{\boldsymbol{w}}_{3_i} - d_i\Omega_i^2\hat{\boldsymbol{w}}_{2_i} \tag{7}$$

missing term ???

Using the transport theorem [14,17] or cross product rule that relates time derivatives as seen by different frames, the inertial and body-relative time derivatives of $\boldsymbol{c}$ are related through

$$\ddot{\boldsymbol{c}} = \boldsymbol{c}'' + 2\boldsymbol{\omega}_{\mathcal{B}/\mathcal{N}} \times \boldsymbol{c}' + \dot{\boldsymbol{\omega}}_{\mathcal{B}/\mathcal{N}} \times \boldsymbol{c} + \boldsymbol{\omega}_{\mathcal{B}/\mathcal{N}} \times (\boldsymbol{\omega}_{\mathcal{B}/\mathcal{N}} \times \boldsymbol{c}) \tag{8}$$

Substituting Eqs. (1), (7), and (8) into Eq. (2) and grouping second-order terms on the left-hand side yields the translational equation of motion.

$$m_{\text{sc}}\ddot{\boldsymbol{r}}_{B/N} - m_{\text{sc}}[\tilde{\boldsymbol{c}}]\dot{\boldsymbol{\omega}}_{\mathcal{B}/\mathcal{N}} + \sum_{i=1}^{N_{\text{rw}}} m_{\text{rw}_i}d_i\hat{\boldsymbol{w}}_{3_i}\dot{\Omega}_i = \boldsymbol{F} - 2m_{\text{sc}}[\tilde{\boldsymbol{\omega}}_{\mathcal{B}/\mathcal{N}}]\boldsymbol{c}' - m_{\text{sc}}[\tilde{\boldsymbol{\omega}}_{\mathcal{B}/\mathcal{N}}][\tilde{\boldsymbol{\omega}}_{\mathcal{B}/\mathcal{N}}]\boldsymbol{c} + \sum_{i=1}^{N_{\text{rw}}} m_{\text{rw}_i}d_i\Omega_i^2\hat{\boldsymbol{w}}_{2_i} \tag{9}$$

Note that the tilde operator designates the skew symmetric matrix, that is, $[\tilde{\boldsymbol{c}}]\boldsymbol{v} \equiv \boldsymbol{c} \times \boldsymbol{v}$. Additionally this notation is still frame independent as no specific frame is designated and represents the vector cross product operation in a compact manner. Equation (9) shows that the translational acceleration, $\ddot{\boldsymbol{r}}_{B/N}$, is coupled with the rotational acceleration, $\dot{\boldsymbol{\omega}}_{\mathcal{B}/\mathcal{N}}$, and the wheel accelerations, $\dot{\Omega}_i$. This is a result of the fact that the RWs are imbalanced and therefore change the center of mass location of the spacecraft [14].

B. Rotational Motion

Next the rotational spacecraft EOMs are developed. This derivation starts with the inertial angular momentum of the total spacecraft about the general body-fixed point B:

$$\boldsymbol{H}_{\text{sc},B} = \boldsymbol{H}_{\text{hub},B} + \sum_{i=1}^{N_{\text{rw}}} \boldsymbol{H}_{\text{rw}_i,B} \tag{10}$$

The spacecraft hub and RW angular momentum expressions about point B are written relating them to the angular momentum about their respective center of mass locations B_c and W_{c_i} as

$$\boldsymbol{H}_{\text{hub},B} = [I_{\text{hub},B_c}]\boldsymbol{\omega}_{\mathcal{B}/\mathcal{N}} + m_{\text{hub}}\boldsymbol{r}_{B_c/B} \times \dot{\boldsymbol{r}}_{B_c/B} \tag{11}$$

$$\boldsymbol{H}_{\text{rw}_i,B} = [I_{\text{rw}_i,W_{c_i}}](\boldsymbol{\omega}_{\mathcal{B}/\mathcal{N}} + \Omega_i\hat{\boldsymbol{g}}_{s_i}) + m_{\text{rw}_i}\boldsymbol{r}_{W_{c_i}/B} \times \dot{\boldsymbol{r}}_{W_{c_i}/B} \tag{12}$$

The first step to develop the desired rotational EOMs is to take the inertial time derivative of the system angular momentum vector about point B [14].

$$\dot{\boldsymbol{H}}_{\text{sc},B} = \boldsymbol{L}_B + m_{\text{sc}}\ddot{\boldsymbol{r}}_{B/N} \times \boldsymbol{c} \tag{13}$$

The left-hand side of Eq. (13) is found by taking the inertial time derivative of Eq. (10).

$$\dot{\boldsymbol{H}}_{\text{sc},B} = \dot{\boldsymbol{H}}_{\text{hub},B} + \sum_{i=1}^{N_{\text{rw}}} \dot{\boldsymbol{H}}_{\text{rw}_i,B} \tag{14}$$

Taking the inertial time derivative of Eq. (11) while using the transport theorem yields

$$\dot{\boldsymbol{H}}_{\text{hub},B} = [I_{\text{hub},B_c}]\dot{\boldsymbol{\omega}}_{\mathcal{B}/\mathcal{N}} + \boldsymbol{\omega}_{\mathcal{B}/\mathcal{N}} \times [I_{\text{hub},B_c}]\boldsymbol{\omega}_{\mathcal{B}/\mathcal{N}} + m_{\text{hub}}\boldsymbol{r}_{B_c/B} \times \ddot{\boldsymbol{r}}_{B_c/B} \tag{15}$$

Noting that $\boldsymbol{r}_{B_c/B}$ is a body-fixed vector yields the following second-order inertial time derivative is

$$\ddot{\boldsymbol{r}}_{B_c/B} = \dot{\boldsymbol{\omega}}_{\mathcal{B}/\mathcal{N}} \times \boldsymbol{r}_{B_c/B} + \boldsymbol{\omega}_{\mathcal{B}/\mathcal{N}} \times (\boldsymbol{\omega}_{\mathcal{B}/\mathcal{N}} \times \boldsymbol{r}_{B_c/B}) \tag{16}$$

Substituting Eq. (16) into Eq. (15) and simplifying yields

$$\dot{\boldsymbol{H}}_{\text{hub},B} = [I_{\text{hub},B_c}]\dot{\boldsymbol{\omega}}_{\mathcal{B}/\mathcal{N}} + \boldsymbol{\omega}_{\mathcal{B}/\mathcal{N}} \times [I_{\text{hub},B_c}]\boldsymbol{\omega}_{\mathcal{B}/\mathcal{N}} + m_{\text{hub}}\boldsymbol{r}_{B_c/B} \times (\dot{\boldsymbol{\omega}}_{\mathcal{B}/\mathcal{N}} \times \boldsymbol{r}_{B_c/B}) + m_{\text{hub}}\boldsymbol{r}_{B_c/B} \times (\boldsymbol{\omega}_{\mathcal{B}/\mathcal{N}} \times (\boldsymbol{\omega}_{\mathcal{B}/\mathcal{N}} \times \boldsymbol{r}_{B_c/B})) \tag{17}$$

Employing the Jacobi triple-product identity, $\boldsymbol{a}\times(\boldsymbol{b}\times\boldsymbol{c}) = (\boldsymbol{a}\times\boldsymbol{b})\times\boldsymbol{c} + \boldsymbol{b}\times(\boldsymbol{a}\times\boldsymbol{c})$, on the right-hand side of Eq. (17) and using the parallel axis theorem,

$$[I_{\text{hub},B}] = [I_{\text{hub},B_c}] + m_{\text{hub}}[\tilde{\boldsymbol{r}}_{B_c/B}][\tilde{\boldsymbol{r}}_{B_c/B}]^T \tag{18}$$

the hub angular momentum derivative is finally written compactly as

$$\dot{\boldsymbol{H}}_{\text{hub},B} = [I_{\text{hub},B}]\dot{\boldsymbol{\omega}}_{\mathcal{B}/\mathcal{N}} + [\tilde{\boldsymbol{\omega}}_{\mathcal{B}/\mathcal{N}}][I_{\text{hub},B}]\boldsymbol{\omega}_{\mathcal{B}/\mathcal{N}} \tag{19}$$

In the above expression it is assumed that all matrix representations are taken with respect to a consistent reference frame. However, as this frame is not specified, this compact matrix notation is still frame independent.

Following an equivalent derivation procedure, the inertial time derivative of RW angular momentum about point B is

$$\dot{\boldsymbol{H}}_{\text{rw}_i,B} = [I_{\text{rw}_i,W_{c_i}}]'(\boldsymbol{\omega}_{\mathcal{B}/\mathcal{N}} + \Omega_i\hat{\boldsymbol{g}}_{s_i}) + [I_{\text{rw}_i,W_{c_i}}](\dot{\boldsymbol{\omega}}_{\mathcal{B}/\mathcal{N}} + \dot{\Omega}_i\hat{\boldsymbol{g}}_{s_i}) + \boldsymbol{\omega}_{\mathcal{B}/\mathcal{N}}\times[I_{\text{rw}_i,W_{c_i}}](\boldsymbol{\omega}_{\mathcal{B}/\mathcal{N}} + \Omega_i\hat{\boldsymbol{g}}_{s_i}) + m_{\text{rw}_i}\boldsymbol{r}_{W_{c_i}/B}\times\ddot{\boldsymbol{r}}_{W_{c_i}/B} \tag{20}$$

trans port thm

To simplify the $[I_{\text{rw}_i,W_{c_i}}]'$ expression, the RW inertia tensor $[I_{\text{rw}_i/W_{c_i}}]$ is defined in its most general form using the $\mathcal{W}_i$ frame base vectors as

$$[I_{\text{rw}_i/W_{c_i}}] = J_{11_i}\hat{\boldsymbol{g}}_{s_i}\hat{\boldsymbol{g}}_{s_i}^T + J_{12_i}\hat{\boldsymbol{g}}_{s_i}\hat{\boldsymbol{w}}_{2_i}^T + J_{13_i}\hat{\boldsymbol{g}}_{s_i}\hat{\boldsymbol{w}}_{3_i}^T + J_{12_i}\hat{\boldsymbol{w}}_{2_i}\hat{\boldsymbol{g}}_{s_i}^T + J_{22_i}\hat{\boldsymbol{w}}_{2_i}\hat{\boldsymbol{w}}_{2_i}^T + J_{23_i}\hat{\boldsymbol{w}}_{2_i}\hat{\boldsymbol{w}}_{3_i}^T + J_{13_i}\hat{\boldsymbol{w}}_{3_i}\hat{\boldsymbol{g}}_{s_i}^T + J_{23_i}\hat{\boldsymbol{w}}_{3_i}\hat{\boldsymbol{w}}_{2_i}^T + J_{33_i}\hat{\boldsymbol{w}}_{3_i}\hat{\boldsymbol{w}}_{3_i}^T \tag{21}$$

?

Note that in Eq. (21) the vector outerproduct between two vectors $\boldsymbol{a}$ and $\boldsymbol{b}$ is defined compactly in matrix form as $\boldsymbol{a}\boldsymbol{b}^T$. As no specific frame designation is applied in this notation, and vectors $\boldsymbol{a}$ and $\boldsymbol{b}$ must simply be expressed with respect to the same frame to evaluate $\boldsymbol{a}\boldsymbol{b}^T$, this formulation is frame independent. The definition of $[I_{\text{rw}_i/W_{c_i}}]$ allows for any RW inertia matrix definition to be considered. Section IV describes the characterization of the dynamic imbalance of the RW by defining parameters in $[I_{\text{rw}_i/W_{c_i}}]$.

The body-frame derivatives of wheel-frame basis vectors are

$$\hat{\boldsymbol{g}}_{s_i}' = 0 \quad \hat{\boldsymbol{w}}_{2_i}' = \Omega_i\hat{\boldsymbol{w}}_{3_i} \quad \hat{\boldsymbol{w}}_{3_i}' = -\Omega_i\hat{\boldsymbol{w}}_{2_i} \tag{22}$$

Taking the $\mathcal{B}$-frame time derivative of $[I_{\text{rw}_i/W_{c_i}}]$ while using the transport theorem yields

$$^{\mathcal{W}_i}[I_{\text{rw}_i/W_{c_i}}]' = \begin{array}{c} ^{\mathcal{W}_i} \\ \end{array}\begin{bmatrix} 0 & -J_{13_i} & J_{12_i} \\ -J_{13_i} & -2J_{23_i} & J_{22_i} - J_{33_i} \\ J_{12_i} & J_{22_i} - J_{33_i} & 2J_{23_i} \end{bmatrix}\Omega_i \tag{23}$$

In the above matrix notation the left-superscript symbol denotes with respect to which frame the inertia tensor components are evaluated.

The remaining term in Eq. (20) that needs to be defined is $\ddot{\boldsymbol{r}}_{W_{c_i}/B}$. The RW wheel center of mass location W_{c_i} relative to body-fixed point B is

$$\boldsymbol{r}_{W_{c_i}/B} = \boldsymbol{r}_{W_i/B} + d_i\hat{\boldsymbol{w}}_{2_i} \tag{24}$$

The second-order inertial time derivative of this vector is ... $m\, r \times \ddot{r} = \dot{H}$

$$\ddot{\boldsymbol{r}}_{W_{c_i}/B} = d_i\dot{\Omega}_i\hat{\boldsymbol{w}}_{3_i} - d_i\Omega_i^2\hat{\boldsymbol{w}}_{2_i} + \dot{\boldsymbol{\omega}}_{\mathcal{B}/\mathcal{N}}\times\boldsymbol{r}_{W_{c_i}/B} + 2\boldsymbol{\omega}_{\mathcal{B}/\mathcal{N}}\times d_i\Omega_i\hat{\boldsymbol{w}}_{3_i} + \boldsymbol{\omega}_{\mathcal{B}/\mathcal{N}}\times(\boldsymbol{\omega}_{\mathcal{B}/\mathcal{N}}\times\boldsymbol{r}_{W_{c_i}/B}) \tag{25}$$

Using Eq. (5) and applying the triple-product identity and parallel axis theorem

$$[I_{\text{rw}_i,B}] = [I_{\text{rw}_i,W_{c_i}}] + m_{\text{rw}_i}[\tilde{\boldsymbol{r}}_{W_{c_i}/B}][\tilde{\boldsymbol{r}}_{W_{c_i}/B}]^T \tag{26}$$

results in

$$\dot{\boldsymbol{H}}_{\text{rw}_i,B} = [I_{\text{rw}_i,B}]'\boldsymbol{\omega}_{\mathcal{B}/\mathcal{N}} + [I_{\text{rw}_i,B}]\dot{\boldsymbol{\omega}}_{\mathcal{B}/\mathcal{N}} + [\tilde{\boldsymbol{\omega}}_{\mathcal{B}/\mathcal{N}}][I_{\text{rw}_i,B}]\boldsymbol{\omega}_{\mathcal{B}/\mathcal{N}} + [I_{\text{rw}_i,W_{c_i}}]'\Omega_i\hat{\boldsymbol{g}}_{s_i} + [I_{\text{rw}_i,W_{c_i}}]\dot{\Omega}_i\hat{\boldsymbol{g}}_{s_i} + [\tilde{\boldsymbol{\omega}}_{\mathcal{B}/\mathcal{N}}][I_{\text{rw}_i,W_{c_i}}]\Omega_i\hat{\boldsymbol{g}}_{s_i} + m_{\text{rw}_i}\boldsymbol{r}_{W_{c_i}/B}\times(d_i\dot{\Omega}_i\hat{\boldsymbol{w}}_{3_i} - d_i\Omega_i^2\hat{\boldsymbol{w}}_{2_i}) + m_{\text{rw}_i}\boldsymbol{\omega}_{\mathcal{B}/\mathcal{N}}\times(\boldsymbol{r}_{W_{c_i}/B}\times\boldsymbol{r}'_{W_{c_i}/B}) \tag{27}$$

Note that taking the body-relative time derivative of Eq. (26) yields

$$[I_{\text{rw}_i,B}]' = [I_{\text{rw}_i,W_{c_i}}]' + m_{\text{rw}_i}[\tilde{\boldsymbol{r}}'_{W_{c_i}/B}][\tilde{\boldsymbol{r}}_{W_{c_i}/B}]^T + m_{\text{rw}_i}[\tilde{\boldsymbol{r}}_{W_{c_i}/B}][\tilde{\boldsymbol{r}}'_{W_{c_i}/B}]^T \tag{28}$$

Now the definition of the inertial time derivatives of the hub's angular momentum and RWs' angular momentum, Eqs. (19) and (27), respectively, are substituted into Eq. (14) while making use of $[I_{\text{sc},B}] = [I_{\text{hub},B}] + \sum_{i=1}^{N_{\text{rw}}}[I_{\text{rw}_i,B}]$ to yield

$$\dot{\boldsymbol{H}}_{\text{sc},B} = [I_{\text{sc},B}]\dot{\boldsymbol{\omega}}_{\mathcal{B}/\mathcal{N}} + [\tilde{\boldsymbol{\omega}}_{\mathcal{B}/\mathcal{N}}][I_{\text{sc},B}]\boldsymbol{\omega}_{\mathcal{B}/\mathcal{N}} + [I_{\text{sc},B}]'\boldsymbol{\omega}_{\mathcal{B}/\mathcal{N}} + \sum_{i=1}^{N_{\text{rw}}}\Big[[I_{\text{rw}_i,W_{c_i}}]'\Omega_i\hat{\boldsymbol{g}}_{s_i} + [I_{\text{rw}_i,W_{c_i}}]\dot{\Omega}_i\hat{\boldsymbol{g}}_{s_i} + [\tilde{\boldsymbol{\omega}}_{\mathcal{B}/\mathcal{N}}]([I_{\text{rw}_i,W_{c_i}}]\Omega_i\hat{\boldsymbol{g}}_{s_i} + m_{\text{rw}_i}[\tilde{\boldsymbol{r}}_{W_{c_i}/B}]\boldsymbol{r}'_{W_{c_i}/B}) + m_{\text{rw}_i}[\tilde{\boldsymbol{r}}_{W_{c_i}/B}](d_i\dot{\Omega}_i\hat{\boldsymbol{w}}_{3_i} - d_i\Omega_i^2\hat{\boldsymbol{w}}_{2_i})\Big] \tag{29}$$

Finally Eq. (29) is substituted into Eq. (13) to the additional EOMs:

$$m_{\text{sc}}[\tilde{\boldsymbol{c}}]\ddot{\boldsymbol{r}}_{B/N} + [I_{\text{sc},B}]\dot{\boldsymbol{\omega}}_{\mathcal{B}/\mathcal{N}} + \sum_{i=1}^{N_{\text{rw}}}([I_{\text{rw}_i,W_{c_i}}]\hat{\boldsymbol{g}}_{s_i} + m_{\text{rw}_i}d_i[\tilde{\boldsymbol{r}}_{W_{c_i}/B}]\hat{\boldsymbol{w}}_{3_i})\dot{\Omega}_i = \sum_{i=1}^{N_{\text{rw}}}\Big[m_{\text{rw}_i}[\tilde{\boldsymbol{r}}_{W_{c_i}/B}]d_i\Omega_i^2\hat{\boldsymbol{w}}_{2_i} - [\tilde{\boldsymbol{\omega}}_{\mathcal{B}/\mathcal{N}}]([I_{\text{rw}_i,W_{c_i}}]\Omega_i\hat{\boldsymbol{g}}_{s_i} + m_{\text{rw}_i}[\tilde{\boldsymbol{r}}_{W_{c_i}/B}]\boldsymbol{r}'_{W_{c_i}/B}) - [I_{\text{rw}_i,W_{c_i}}]'\Omega_i\hat{\boldsymbol{g}}_{s_i}\Big] - [\tilde{\boldsymbol{\omega}}_{\mathcal{B}/\mathcal{N}}][I_{\text{sc},B}]\boldsymbol{\omega}_{\mathcal{B}/\mathcal{N}} - [I_{\text{sc},B}]'\boldsymbol{\omega}_{\mathcal{B}/\mathcal{N}} + \boldsymbol{L}_B \tag{30}$$

Equation (30) shows that the rotational EOM is coupled with the other second-order variables. Similar to the translational EOM, this coupling is because the center of mass of the spacecraft is not coincident with point B. The motor torque equation is the remaining necessary EOM to describe the motion of the spacecraft and is defined in the following section.

C. Motor Torque Equation

The motor torque u_{s_i} is the spin axis component of wheel torque about point W_i. The transverse torques acting on the wheel $\tau_{w_{2_i}}$ and $\tau_{w_{3_i}}$ are structural torques on the wheel and do not contribute to the motor torque equation.

$$\boldsymbol{L}_{W_i} = \boxed{u_{s_i}\hat{\boldsymbol{g}}_{s_i}} + \tau_{w_{2_i}}\hat{\boldsymbol{w}}_{2_i} + \tau_{w_{3_i}}\hat{\boldsymbol{w}}_{3_i} \tag{31}$$

The motor torque equation describes how the RW motor torque u_{s_i} relates to the wheel speed derivative $\dot{\Omega}_i$.

Torque about point W_i relates to torque about W_{c_i} by [14]

$$\boldsymbol{L}_{W_i} = \boldsymbol{L}_{W_{c_i}} + \boldsymbol{r}_{W_{c_i}/W_i}\times m_{\text{rw}_i}\ddot{\boldsymbol{r}}_{W_{c_i}/N} \tag{32}$$

As W_{c_i} is the RW wheel center of mass, Euler's equation [14] applies as follows.

$$\boldsymbol{L}_{W_{c_i}} = \dot{\boldsymbol{H}}_{\text{rw}_i,W_{c_i}} \tag{33}$$

The RW angular momentum about W_{c_i} is expressed as

$$\boldsymbol{H}_{\text{rw}_i,W_{c_i}} = [I_{\text{rw}_i,W_{c_i}}]\boldsymbol{\omega}_{\mathcal{W}_i/\mathcal{N}} = [I_{\text{rw}_i,W_{c_i}}](\boldsymbol{\omega}_{\mathcal{B}/\mathcal{N}} + \boldsymbol{\Omega}_i\hat{\boldsymbol{g}}_{s_i}) \tag{34}$$

Note that the $\mathcal{W}_i$ frame components of $\boldsymbol{\omega}_{\mathcal{B}/\mathcal{N}}$ and their corresponding derivatives are defined as

$$\omega_{s_i} = \hat{\boldsymbol{g}}_{s_i}^T \boldsymbol{\omega}_{\mathcal{B}/\mathcal{N}}, \quad \omega_{w_{2_i}} = \hat{\boldsymbol{w}}_{2_i}^T \boldsymbol{\omega}_{\mathcal{B}/\mathcal{N}}, \quad \omega_{w_{3_i}} = \hat{\boldsymbol{w}}_{3_i}^T \boldsymbol{\omega}_{\mathcal{B}/\mathcal{N}} \tag{35}$$

$$\dot{\omega}_{s_i} = \hat{\boldsymbol{g}}_{s_i}^T \dot{\boldsymbol{\omega}}_{\mathcal{B}/\mathcal{N}}, \ \dot{\omega}_{w_{2_i}} = \hat{\boldsymbol{w}}_{2_i}^T \dot{\boldsymbol{\omega}}_{\mathcal{B}/\mathcal{N}} + \Omega_i \omega_{w_{3_i}}, \ \dot{\omega}_{w_{3_i}} = \hat{\boldsymbol{w}}_{3_i}^T \dot{\boldsymbol{\omega}}_{\mathcal{B}/\mathcal{N}} - \Omega_i \omega_{w_{2_i}} \tag{36}$$

To aid in the simplification of the motor torque equation, $[I_{\text{rw}_i, W_{c_i}}]$ is expressed as an outer product sum as in Eq. (21) and substituted into Eq. (34) to yield

$$\begin{aligned} \boldsymbol{H}_{\text{rw}_i, W_{c_i}} &= (J_{11_i}\omega_{s_i} + J_{11_i}\Omega_i + J_{12_i}\omega_{w_{2_i}} + J_{13_i}\omega_{w_{3_i}})\hat{\boldsymbol{g}}_{s_i} \\ &+ (J_{12_i}\omega_{s_i} + J_{12_i}\Omega_i + J_{22_i}\omega_{w_{2_i}} + J_{23_i}\omega_{w_{3_i}})\hat{\boldsymbol{w}}_{2_i} \\ &+ (J_{13_i}\omega_{s_i} + J_{13_i}\Omega_i + J_{23_i}\omega_{w_{2_i}} + J_{33_i}\omega_{w_{3_i}})\hat{\boldsymbol{w}}_{3_i} \end{aligned} \tag{37}$$

Taking the inertial derivative of the wheel angular momentum about W_c in Eq. (37) gives

$$\begin{aligned} \dot{\boldsymbol{H}}_{\text{rw}_i, W_{c_i}} &= [(J_{11_i}\hat{\boldsymbol{g}}_{s_i}^T + J_{12_i}\hat{\boldsymbol{w}}_{2_i}^T + J_{13_i}\hat{\boldsymbol{w}}_{3_i}^T)\dot{\boldsymbol{\omega}}_{\mathcal{B}/\mathcal{N}} + J_{11_i}\dot{\Omega}_i \\ &+ \omega_{s_i}(J_{13_i}\omega_{w_{2_i}} - J_{12_i}\omega_{w_{3_i}}) + \omega_{w_{3_i}}\omega_{w_{2_i}}(J_{33_i} - J_{22_i}) \\ &+ J_{23_i}(\omega_{w_{2_i}}^2 - \omega_{w_{3_i}}^2)]\hat{\boldsymbol{g}}_{s_i} + P_i\hat{\boldsymbol{w}}_{2_i} + Q_i\hat{\boldsymbol{w}}_{3_i} \end{aligned} \tag{38}$$

The scalar quantities P_i and Q_i are the coefficients of $\ddot{\boldsymbol{H}}_{\text{rw}_i, W_{c_i}}$ along $\hat{\boldsymbol{w}}_{2_i}$ and $\hat{\boldsymbol{w}}_{3_i}$, respectively. Because only the coefficient of $\hat{\boldsymbol{g}}_{s_i}$ relates to the motor torque equation as in Eqs. (31) and (32), specifying P_i and Q_i is unnecessary as they do not contribute to the RW motor torque u_{s_i}.

The next step is to define the remaining terms in Eq. (32). This begins by determining the second inertial derivative of $\ddot{\boldsymbol{r}}_{W_{c_i}/N} = \ddot{\boldsymbol{r}}_{B/N} + \ddot{\boldsymbol{r}}_{W_{c_i}/B}$. Each cross product in Eq. (25) is evaluated using wheel-frame base vectors. For example,

$$(\boldsymbol{\omega}_{\mathcal{B}/\mathcal{N}} + \Omega_i\hat{\boldsymbol{g}}_{s_i}) \times d_i\hat{\boldsymbol{w}}_{2_i} = -d_i\omega_{w_{3_i}}\hat{\boldsymbol{g}}_{s_i} + d_i(\omega_{s_i} + \Omega_i)\hat{\boldsymbol{w}}_{3_i} \tag{39}$$

Repeating this procedure yields the following expression for the right-hand term of Eq. (32). Note that the scalar term R_i is the derivative component along $\hat{\boldsymbol{w}}_{3_i}$ and does need to be defined because only the $\hat{\boldsymbol{g}}_{s_i}$ component is desired.

$$\begin{aligned} \boldsymbol{r}_{W_{c_i}/W_i} \times m_{\text{rw}_i}\ddot{\boldsymbol{r}}_{W_{c_i}/N} &= m_{\text{rw}_i}d_i[\hat{\boldsymbol{w}}_{3_i}^T\ddot{\boldsymbol{r}}_{B/N} - \hat{\boldsymbol{w}}_{3_i}^T[\tilde{\boldsymbol{r}}_{W_i/B}]\dot{\boldsymbol{\omega}}_{\mathcal{B}/\mathcal{N}} \\ &+ \hat{\boldsymbol{w}}_{3_i}^T[\tilde{\boldsymbol{\omega}}_{\mathcal{B}/\mathcal{N}}][\tilde{\boldsymbol{\omega}}_{\mathcal{B}/\mathcal{N}}]\boldsymbol{r}_{W_i/B} + d_i(\hat{\boldsymbol{g}}_{s_i}^T\dot{\boldsymbol{\omega}}_{\mathcal{B}/\mathcal{N}} + \dot{\Omega}_i) \\ &+ d_i\omega_{w_{2_i}}\omega_{w_{3_i}}]\hat{\boldsymbol{g}}_{s_i} - R_i\hat{\boldsymbol{w}}_{3_i} \end{aligned} \tag{40}$$

The scalar motor torque equation for each RW is obtained by summing the $\hat{\boldsymbol{g}}_{s_i}$ components of Eq. (38) and Eq. (40) and simplifying to yield

$$\begin{aligned} &[m_{\text{rw}_i}d_i\hat{\boldsymbol{w}}_{3_i}^T]\ddot{\boldsymbol{r}}_{B/N} + [(J_{11_i} + m_{\text{rw}_i}d_i^2)\hat{\boldsymbol{g}}_{s_i}^T + J_{12_i}\hat{\boldsymbol{w}}_{2_i}^T + J_{13_i}\hat{\boldsymbol{w}}_{3_i}^T \\ &- m_{\text{rw}_i}d_i\hat{\boldsymbol{w}}_{3_i}^T[\tilde{\boldsymbol{r}}_{W_i/B}]]\dot{\boldsymbol{\omega}}_{\mathcal{B}/\mathcal{N}} + [J_{11_i} + m_{\text{rw}_i}d_i^2]\dot{\Omega}_i = J_{23_i}(\omega_{w_{3_i}}^2 - \omega_{w_{2_i}}^2) \\ &+ \omega_{s_i}(J_{12_i}\omega_{w_{3_i}} - J_{13_i}\omega_{w_{2_i}}) + \omega_{w_{2_i}}\omega_{w_{3_i}}(J_{22_i} - J_{33_i} - m_{\text{rw}_i}d_i^2) \\ &- m_{\text{rw}_i}d_i\hat{\boldsymbol{w}}_{3_i}^T[\tilde{\boldsymbol{\omega}}_{\mathcal{B}/\mathcal{N}}][\tilde{\boldsymbol{\omega}}_{\mathcal{B}/\mathcal{N}}]\boldsymbol{r}_{W_i/B} + u_{s_i} \end{aligned} \tag{41}$$

As a form of validation, the balanced motor torque equation may be obtained by zeroing out all imbalance terms $(d_i, J_{12_i}, J_{13_i}, J_{23_i})$ and making the assumption $J_{22_i} = J_{33_i}$. Under these conditions, Eq. (41) is simplified to the expected balanced RW motor torque equation [14]

$$u_{s_i} = J_{11_i}(\hat{\boldsymbol{g}}_{s_i}^T\dot{\boldsymbol{\omega}}_{\mathcal{B}/\mathcal{N}} + \dot{\Omega}_i) \tag{42}$$

This concludes the necessary derivations for the fully coupled EOMs of a spacecraft with RWs containing static and dynamic imbalances. The EOMs in Eqs. (9), (30), and (41) provide the required $6 + N_{\text{rw}}$ differential equations to fully define the dynamic response.

IV. Imbalance Parameter Adaptation

Because the simplified RW jitter model [8] assumes an external force and torque on the spacecraft, the EOMs for the fully coupled model and the simplified RW jitter model are significantly more complex to formulate and implement. However, due to the coupled nature of the EOMs, the equivalent terms in the simplified model compared with the first-principles model are not readily apparent in EOMs presented thus far. This section investigates which terms in the fully coupled solution are equivalent to the simplified disturbance model terms. This allows static and dynamic imbalance parameters, typically available from an RW manufacturer, to be readily applied to the fully coupled model.

A. Overview of Existing Simplified Static and Dynamic Imbalance Model

The well-established method to specify the imbalanced RW motion is to lump sources of imbalance into scalar parameters. The simplified RW imbalance model directly uses such specifications to model jitter as an external torque [3,8]. The static imbalance component is due to the RW wheel center of mass not being on the rotation axis $\hat{\boldsymbol{g}}_{s_i}$. This is specified by the parameter U_{s_i}, typically given in units of $\text{g} \cdot \text{cm}$. The static imbalance is thus approximated through an external force $\boldsymbol{F}_{s_i}$ defined as

$$\boldsymbol{F}_{s_i} = U_{s_i}\Omega_i^2\hat{\boldsymbol{u}}_i \tag{43}$$

where $\hat{\boldsymbol{u}}_i$ is an arbitrary unit vector normal to the wheel spin axis. If the RW is not coincident with the spacecraft center of mass, torque on the spacecraft resulting from the static imbalance force is given by the simplified model as

$$\boldsymbol{L}_{s_i} = \boldsymbol{r}_{W_i/B} \times \boldsymbol{F}_{s_i} = U_{s_i}\Omega_i^2[\tilde{\boldsymbol{r}}_{W_i/B}]\hat{\boldsymbol{u}}_i \tag{44}$$

Note that the simplified model uses the approximation $\boldsymbol{r}_{W_{c_i}/B} \approx \boldsymbol{r}_{W_i/B}$ since d_i is small.

Dynamic imbalance is due to the wheel principal inertia axes not being aligned with the spin axis $\hat{\boldsymbol{g}}_{s_i}$. This is specified by the parameter U_d, typically given in units $\text{g} \cdot \text{cm}^2$. The dynamic imbalance component is thus approximated through an external torque $\boldsymbol{L}_{d_i}$ defined as

$$\boldsymbol{L}_{d_i} = U_{d_i}\Omega_i^2\hat{\boldsymbol{v}}_i \tag{45}$$

where $\hat{\boldsymbol{v}}_i$ is an arbitrary unit vector normal to the wheel spin axis. Note that $\hat{\boldsymbol{u}}_i$ and $\hat{\boldsymbol{v}}_i$ are only required to be normal to their corresponding spin axis $\hat{\boldsymbol{g}}_{s_i}$. This is because the lumped parameters U_{s_i} and U_{d_i} do not contain any information on orientation/location of mass imbalances about $\hat{\boldsymbol{g}}_{s_i}$. Additionally, the initial value of the wheel angle parameter is arbitrarily chosen, which further emphasizes the arbitrariness of the vectors $\hat{\boldsymbol{u}}_i$ and $\hat{\boldsymbol{v}}_i$ since they relate to the body frame through wheel angle θ_i.

B. Equivalent Terms in the First-Principles Static and Dynamic Imbalance Model

To relate the simplified model to the first-principles–based model developed within this paper, Eq. (30) is analyzed to identify terms that directly contribute to torque on the spacecraft. The simplified torque in Eq. (44) is proportional to the wheel speed squared and the cross product of wheel location. The first right-hand side term of Eq. (30) is related to the simplified static imbalance model to yield

$$U_{s_i}\Omega_i^2[\tilde{\boldsymbol{r}}_{W/B_i}]\hat{\boldsymbol{u}}_i \quad \leftrightarrow \quad m_{\text{rw}_i}d_i\Omega_i^2[\tilde{\boldsymbol{r}}_{W_{c_i}/B}]\hat{\boldsymbol{w}}_{2_i} \tag{46}$$

Note that $\hat{\boldsymbol{u}}_i$ is arbitrary, but must lie in the $\hat{\boldsymbol{w}}_{2_i}$–$\hat{\boldsymbol{w}}_{3_i}$ plane. Thus, without loss in generality, the assumption that $\hat{\boldsymbol{u}}_i = \hat{\boldsymbol{w}}_{2_i}$ is made. Further, making the simplified model approximation $\boldsymbol{r}_{W_{c_i}/B} \approx \boldsymbol{r}_{W_i/B}$

then yields an expression for d_i in terms of the RW manufacturer–provided static imbalance coefficient U_{s_i} and the wheel mass m_{rw_i}.

$$d_i = \frac{U_{s_i}}{m_{\mathrm{rw}_i}} \tag{47}$$

The simplified dynamic imbalance torque in Eq. (45) is proportional again to the square of the wheel speed, and is in the plane orthogonal to the spin axis $\hat{\boldsymbol{g}}_{s_i}$. Studying again Eq. (30), the last term inside the summation is compared with the simplified dynamic imbalance expression.

$$U_{d_i}\Omega_i^2 \hat{\boldsymbol{v}}_i \;\leftrightarrow\; [I_{\mathrm{rw}_i,W_{c_i}}]'\Omega_i \hat{\boldsymbol{g}}_{s_i} = \Omega_i^2(-J_{13}\hat{\boldsymbol{w}}_{2_i} + J_{12}\hat{\boldsymbol{w}}_{3_i}) \tag{48}$$

As $\hat{\boldsymbol{v}}_i$ is an arbitrary unit direction vector in the $\hat{\boldsymbol{w}}_{2_i}$–$\hat{\boldsymbol{w}}_{3_i}$ plane, taking the norm of Eq. (48) yields the dynamic imbalance manufacturers' parameter U_{d_i}

$$U_{d_i} = \sqrt{J_{13_i}^2 + J_{12_i}^2} \tag{49}$$

in terms of the RW cross-axes inertia's J_{12} and J_{13}. This expression agrees with the relationship found in [3]. Thus, the fully coupled model is underconstrained with respect to the implementation of the simplified model, and some combination of J_{12} and J_{13} must be selected for each wheel such that Eq. (49) is satisfied. Because the unit vector $\hat{\boldsymbol{v}}_i$ is arbitrary (as well as $\hat{\boldsymbol{w}}_{2_i}$ and $\hat{\boldsymbol{w}}_{3_i}$ due to the arbitrariness of initial wheel angle), the following definitions are chosen

$$J_{13_i} = U_{d_i} \tag{50a}$$

$$J_{12_i} = 0 \tag{50b}$$

To complete the discussion of characterizing RW static and dynamic imbalances from manufactures' specifications, the full RW inertia matrix needs to be defined. The balanced RW inertia matrix definition is assumed to be diagonal in the $\mathcal{P}_i$ frame: the principal axes frame of the symmetric RW. The RW wheel principal inertia J_{s_i} is about the axis $\hat{\boldsymbol{g}}_{s_i}$, while the principal inertia J_{t_i} is about the transverse axis orthogonal to $\hat{\boldsymbol{g}}_{s_i}$. For there to only be J_{13_i} terms present in the $\mathcal{W}_i$ representation of the RW's inertia matrix, the direction cosine or rotation matrix between $\mathcal{W}_i$ and $\mathcal{P}_i$, labeled as $[\mathcal{W}_i\mathcal{P}_i]$, must be a single-axis rotation about the $\hat{\boldsymbol{w}}_{2_i}$ axis, where β_i is the angle of rotation. Transforming $[I_{\mathrm{rw}_i,W_{c_i}}]$ from the frame to the $\mathcal{W}_i$ frame and using small angle approximations yields

$$^{\mathcal{W}_i}[I_{\mathrm{rw}_i,W_{c_i}}] = {}^{\mathcal{W}_i}\begin{bmatrix} J_{s_i} & 0 & (J_{s_i}-J_{t_i})\beta_i \\ 0 & J_{t_i} & 0 \\ (J_{s_i}-J_{t_i})\beta_i & 0 & J_{t_i} \end{bmatrix} \tag{51}$$

However, from Eq. (50a), $[I_{\mathrm{rw}_i/W_{c_i}}]$ can be written in the following form:

$$^{\mathcal{W}_i}[I_{\mathrm{rw}_i/W_{c_i}}] = {}^{\mathcal{W}_i}\begin{bmatrix} J_{s_i} & 0 & U_{d_i} \\ 0 & J_{t_i} & 0 \\ U_{d_i} & 0 & J_{t_i} \end{bmatrix} \tag{52}$$

This concludes the necessary steps to relate manufactures' specifications of RW imbalances to parameters needed for the first-principles jitter model. In addition, the simplified description of $[I_{\mathrm{rw}_i/W_{c_i}}]$ seen in Eq. (52) simplifies the EOMs developed in the previous sections due to $J_{12_i} = J_{23_i} = 0$. In addition, Eqs. (47), (50a), and (52) allow a direct comparison of the results of the simplified model to the fully coupled model, which is discussed in the following section.

Table 1 Simulation parameters for the fully coupled model

Parameter	Notation	Value	Units
Number of reaction wheels	N_{rw}	3	——
Total spacecraft mass	m_{sc}	662	kg
Hub mass	m_{hub}	644	kg
Wheel mass	m_{rw}	6	kg
Hub inertia tensor about hub center of mass	$[I_{\mathrm{hub},B_c}]$	$^{\mathcal{B}}\begin{bmatrix} 550 & 0.1045 & -0.0840 \\ 0.1045 & 650 & 0.0001 \\ -0.0840 & 0.0001 & 650 \end{bmatrix}$	$\mathrm{kg \cdot m^2}$
Hub CoM location w.r.t. B	$\boldsymbol{r}_{B_c/B}$	$^{\mathcal{B}}[1 \quad -2 \quad 10]^T$	cm
Wheel orientation matrix	$[G_s]$	$^{\mathcal{B}}\begin{bmatrix} 0.7887 & -0.2113 & -0.5774 \\ -0.2113 & 0.7887 & -0.5774 \\ 0.5774 & 0.5774 & 0.5774 \end{bmatrix}$	——
Wheel static imbalance	U_s	1920	$\mathrm{g \cdot cm}$
Wheel static imbalance	U_d	1540	$\mathrm{g \cdot cm^2}$
Wheel CoM offset (derived from U_s)	d	3.2	mm
Wheel inertia tensor about wheel CoM (derived from U_d)	$[I_{\mathrm{rw},W_c}]$	$^{\mathcal{W}}\begin{bmatrix} 0.0796 & 0 & 2.0E-4 \\ 0 & 0.0430 & 0 \\ 2.0E-4 & 0 & 0.0430 \end{bmatrix}$	$\mathrm{kg \cdot m^2}$
Wheel 1 location vector	$\boldsymbol{r}_{W_1/B}$	$^{\mathcal{B}}[0.6309 \quad -0.1691 \quad 0.4619]^T$	
Wheel 2 location vector	$\boldsymbol{r}_{W_2/B}$	$^{\mathcal{B}}[-0.1691 \quad 0.6309 \quad 0.4619]^T$	
Wheel 3 location vector	$\boldsymbol{r}_{W_3/B}$	$^{\mathcal{B}}[-0.4619 \quad -0.4619 \quad 0.4619]^T$	m
Initial position	$\boldsymbol{r}_{B/N}$	$^{\mathcal{N}}[0 \quad 0 \quad 0]^T$	m
Initial velocity	$\dot{\boldsymbol{r}}_{B/N}$	$^{\mathcal{N}}[0 \quad 0 \quad 0]^T$	m/s
Initial attitude MRP	$\boldsymbol{\sigma}_{\mathcal{B}/\mathcal{N}}$	$[0 \quad 0 \quad 0]^T$	——
Initial angular velocity	$\boldsymbol{\omega}_{\mathcal{B}/\mathcal{N}}$	$^{\mathcal{B}}[0 \quad 0 \quad 0]^T$	deg/s
Initial wheel speeds	Ω	−558, −73, 242	RPM
Initial wheel angles	θ	43, 179, 346	deg
Commanded wheel torques	u_{s_i}	10, −25, 17.5	$\mathrm{mN \cdot m}$

CoM, center of mass.

Note that wheel parameters apply to all wheels unless otherwise specified.

V. Numeric Simulations

Numeric simulations are provided to demonstrate the first-principles–based fully coupled imbalanced RW model developed within this paper. The total angular momentum vector is calculated to confirm that when no external disturbances are present, angular momentum is conserved, and system energy is calculated to show that when no external disturbances or RW motor torques are present, energy is conserved. The fully coupled model is directly compared with the simplified model using the formulation developed in Sec. IV.B. Simulation parameters used are given in Table 1. The wheel orientation matrix $[G_s]$ is of size $3 \times N_{\mathrm{rw}}$ with each column containing the spin axis unit vector for the ith wheel: $[G_s] = [\hat{\boldsymbol{g}}_{s_1} \quad \cdots \quad \hat{\boldsymbol{g}}_{s_{N_{\mathrm{rw}}}}]$. The motor torques u_{s_i} are nominally zero until 3.5 s into the simulation when they assume a 0.5 s constant value listed in Table 1. The numerical integration is performed with a fixed-time step fourth-order Runge–Kutta method using a time step of 0.1 ms. This small time step is chosen to show the integration error to machine precision. Imbalanced RW dynamics are stiff coupled differential equations and therefore require a small step size to show energy and momentum conservation; however, a larger step size can be used and still retain reasonable accuracy. To avoid such small time steps it is also possible to use symplectic integrators to ensure that constraint quantities are conserved. However, to illustrate the validity of the presented imbalanced RW EOMs, the explicit Runge–Kutta integration method is chosen.

The first simulation that is included simulates three RWs. The purpose of this simulation is to show the effect of RW jitter on a spacecraft that is initially inertially fixed, and therefore the only perturbations to the spacecraft will be due to the RW jitter. Accordingly, the spacecraft has no external forces present and has zero initial velocity and zero initial angular velocity. The spacecraft's attitude is parameterized in terms of modified Rodrigues parameters (MRPs) [14,18]; however, it should be noted that the development of the EOMs does not depend on the attitude parameterization; therefore any type can be chosen. The RWs are initially spinning with specified values seen in Table 1.

Figures 3–6 show simulation results for the fully coupled and simplified RW imbalance model with $N_{\mathrm{rw}} = 3$ wheels. In Fig. 3a, the attitude of the spacecraft is shown to be drifting due to the imbalance in the RWs. Note that the simplified model compares well with the fully coupled model angular velocity values in Fig. 3b, illustrating the expected good agreement between the two models as the simplified model is used extensively in mission analysis. Figure 3c illustrates the Euler principal rotation angle [14] between $\mathcal{B}$ and $\mathcal{N}$ for each case with the secular drift removed to better illustrate the jitter impact. The secular drift was found by fitting a fifth-order polynomial to the Euler principal rotation angle and subtracting out the polynomial to form Φ seen in Fig. 3c. This shows that the RW jitter results in a perturbation amplitude of around 8 arc · s. The jitter performance modeling difference between the two models is visible here in that the principal angular displacement magnitudes are noticeably different at times.

The translational position and velocity are shown in Figs. 4a and 4b, respectively. These plots demonstrate that there is a nonzero effect due to RW jitter on the position and velocity of the spacecraft. The position and velocity comparison of the fully coupled model and the simplified model shows that the simplified model is not able to track either position or angular velocity well for the given set of initial conditions. However, it should be noted that the overall translational motion in both cases is small.

The fact that the wheel speed data for the fully coupled model and simplified model agree as shown in Fig. 5a demonstrates that the variation in wheel speed is primarily due to the coupling between the hub's angular velocity and wheel speed.

Figure 6 shows the change in energy and momentum plotted versus time for the fully coupled and simplified models. Energy is plotted for a 3.5 s duration because the motor torque is zero during this time (illustrated in Fig. 5b) and the change in energy should be zero. However, Fig. 6a shows that using the simplified model causes energy

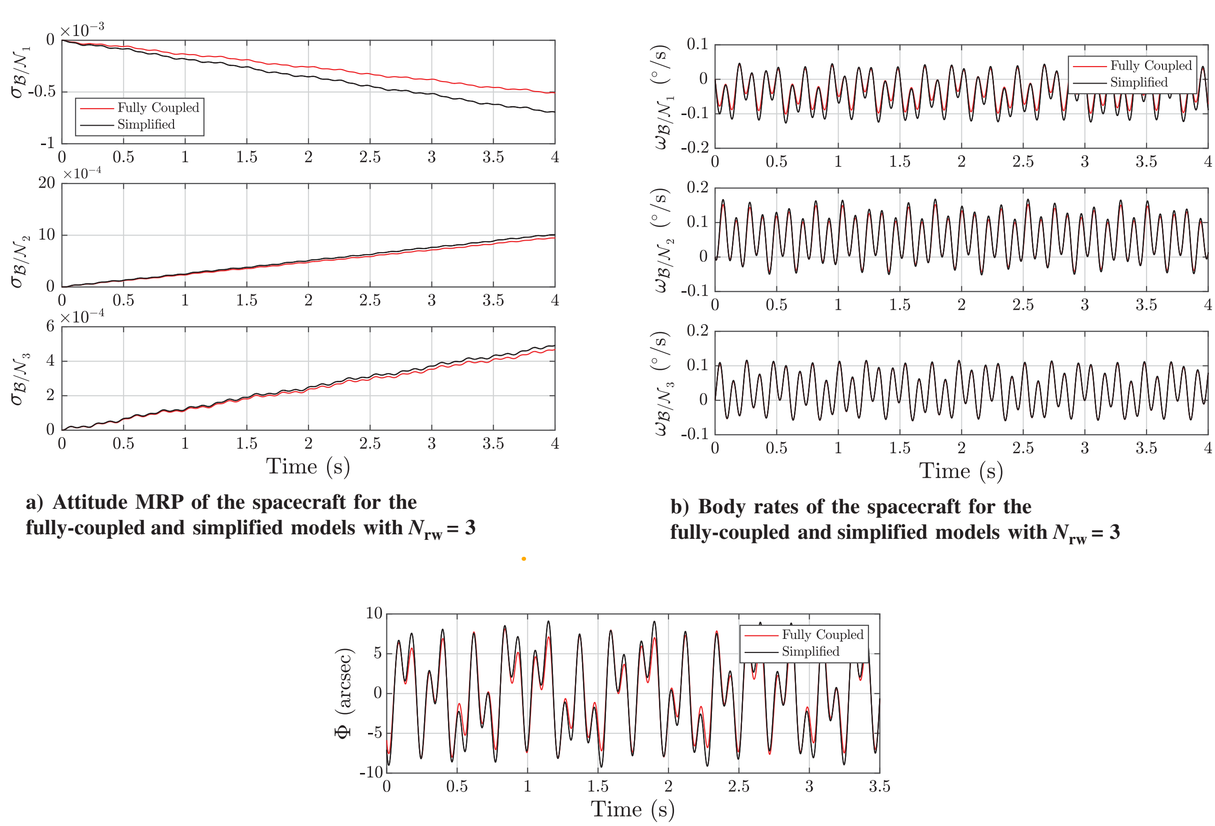

a) Attitude MRP of the spacecraft for the fully-coupled and simplified models with $N_{\mathrm{rw}} = 3$

b) Body rates of the spacecraft for the fully-coupled and simplified models with $N_{\mathrm{rw}} = 3$

c) Principal angle jitter for the fully-coupled and simplified models with $N_{\mathrm{rw}} = 3$

Fig. 3 Attitude, principal angle, and body rates of spacecraft.

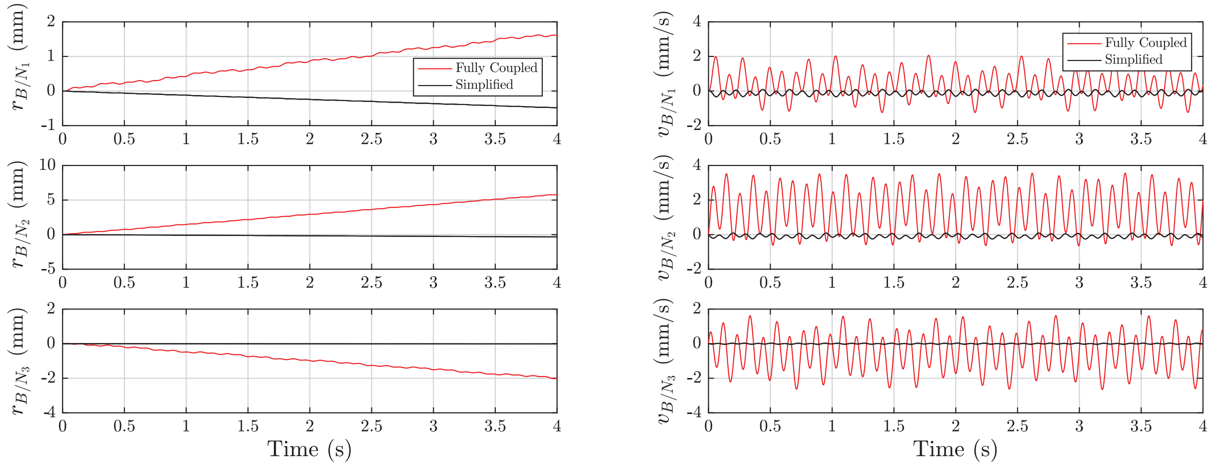

a) Inertial position of the spacecraft for the fully-coupled and simplified models with $N_{rw} = 3$

b) Inertial velocity of the spacecraft for the fully-coupled and simplified models with $N_{rw} = 3$

Fig. 4 Position and velocity of the spacecraft.

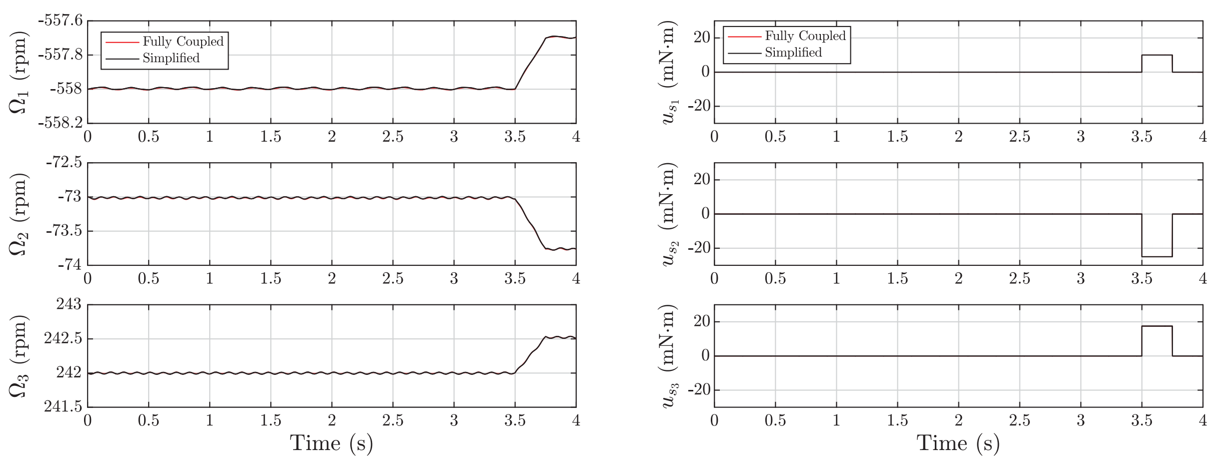

a) Wheel speeds for the fully-coupled and simplified models with $N_{rw} = 3$

b) Open-loop wheel motor torques for the fully-coupled and simplified models with $N_{rw} = 3$

Fig. 5 Wheel angle, wheel speed, and motor torque of RWs.

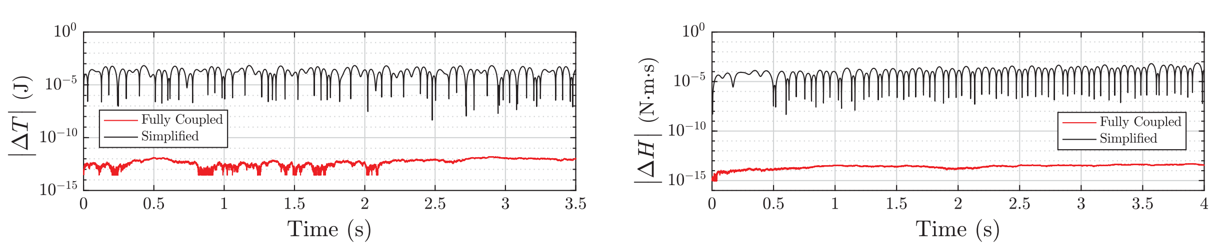

a) System energy Δ for the fully-coupled and simplified models with $N_{rw} = 3$

b) System angular momentum Δ for the fully-coupled and simplified models with $N_{rw} = 3$

Fig. 6 Change in energy and momentum of the spacecraft.

to fluctuate, whereas the fully coupled model includes only integration error. Angular momentum, by definition, should be conserved for a closed system under the influence of internal torques and is thus plotted for the entire duration of the simulation in Fig. 6b. It can be seen that the simplified model violates conservation of angular momentum and the fully coupled model only exhibits integration error. This confirms that the fully coupled model is agreeing with physics and gives confidence that there are no errors in the computer code. However, Figs. 6a and 6b do not provide any verification for the simplified model. If the fully coupled model was not present to compare to, the simplified model would be challenging to verify. This highlights the benefit of this fully coupled model for developing complex spacecraft simulations.

VI. Conclusions

The presented fully coupled first-principles–based RW model with static and dynamic imbalances allows for momentum and energy checks to be implemented in a simulation. Energy is shown to be conserved when the motor torques are zero, and momentum is conserved throughout the length of the simulations. This provides validation of the fully coupled model and highlights drawbacks to the simplified model, which violates conservation of momentum and energy. However, the first-principles–based fully coupled model contains significantly more complex equations to simulate, which results in a more computationally expensive simulation. A comparison between the first-principle–based model and the simplified model shows that the imbalance parameter adaptation is adequate because the fully coupled and simplified models give similar high-level results. However, because the simplified model is not valid in terms of conservation of energy and conservation of angular momentum, it is undesirable when including additional complex dynamical models such as flexible dynamics or fuel slosh. Finally, this fully coupled model can be readily implemented in computer simulation using the well-known manufacturer RW imbalance specifications.

References

[1] Dewell, L., Pedreiro, N., Blaurock, C., Liu, K.-C., Alexander, J., and Levine, M., "Precision Telescope Pointing and Spacecraft Vibration Isolation for the Terrestrial Planet Finder Coronagraph," *Proceedings Volume 5899, UV/Optical/IR Space Telescopes: Innovative Technologies and Concepts II*, Aug. 2005, Paper 589902.
doi:10.1117/12.618939

[2] Rizzo, M., Rinehart, S., Alcorn, J., Barry, R., Benford, D., and Fixsen, D., et al., "Building an Interferometer at the Edge of Space: Pointing and Phase Control System for BETTII," *Proceedings Volume 9143, Space Telescopes and Instrumentation 2014: Optical, Infrared, and Millimeter Wave*, Aug. 2014, Paper 91433H.
doi:10.1117/12.2055016

[3] Markley, F. L., and Crassidis, J. L., *Fundamentals of Spacecraft Attitude Determination and Control*, Space Technology Library, Springer, New York, 2014, pp. 148–152.
doi:10.1007/978-1-4939-0802-8

[4] Park, J., Palazzolo, A., and Beach, R., "MIMO Active Vibration Control of Magnetically Suspended Flywheels for Satellite IPAC Service," *Journal of Dynamic Systems, Measurement, and Control*, Vol. 130, No. 4, 2008, Paper 041005.
doi:10.1115/1.2936846

[5] Park, J., and Palazzolo, A., "Magnetically Suspended VSCMGs for Simultaneous Attitude Control and Power Transfer IPAC Service," *Journal of Dynamic Systems, Measurement, and Control*, Vol. 132, No. 5, 2010, Paper 051001.
doi:10.1115/1.4002105

[6] Masterson, R., Miller, D., and Grogan, R., "Development of Empirical and Analytical Reaction Wheel Disturbance Models," *AIAA Structures, Structural Dynamics, and Materials Conference*, AIAA Paper 1999-1204, 1999.
doi:10.2514/6.1999-1204

[7] Masterson, R., Miller, D., and Grogan, R., "Development and Validation of Reaction Wheel Disturbance Models: Empirical Model," *Journal of Sound and Vibration*, Vol. 249, No. 3, 2002, pp. 575–598.
doi:10.1006/jsvi.2001.3868

[8] Liu, L., "Jitter and Basic Requirements of the Reaction Wheel Assembly in the Attitude Control System," TN, Massachusetts Inst. of Technology, Cambridge, MA, Aug. 2007, http://web.mit.edu/lululiu/Public/TESS%20things/acs_analysis.pdf.

[9] Gutierrez, H., "Performance Assessment and Enhancement of Precision Controlled Structures During Conceptual Design," Ph.D. Dissertation, Dept. of Aeronautics and Astronautics, Massachusetts Inst. of Technology, Cambridge, MA, 1999.

[10] Liu, K.-C., Maghami, P., and Blaurock, C., "Reaction Wheel Disturbance Modeling, Jitter Analysis, and Validation Tests for Solar Dynamics Observatory," *AIAA Guidance, Navigation and Control Conference and Exhibit*, AIAA Paper 2008-7232, 2008.
doi:10.2514/6.2008-7232

[11] Miller, S., Kirchman, P., and Sudey, J., "Reaction Wheel Operational Impacts on the GOES-N Jitter Environment," *AIAA Guidance, Navigation and Control Conference and Exhibit*, AIAA Paper 2007-6736, 2007.
doi:10.2514/6.2007-6736

[12] Kim, D.-K., "Micro-Vibration Model and Parameter Estimation Method of a Reaction Wheel Assembly," *Journal of Sound and Vibration*, Vol. 333, No. 18, 2014, pp. 4214–4231.
doi:10.1016/j.jsv.2014.04.032

[13] Zhang, Y., and Zhang, J., "Disturbance Characteristics Analysis of CMG Due to Imbalances and Installation Errors," *IEEE Transactions on Aerospace and Electronic Systems*, Vol. 50, No. 2, 2014, pp. 1017–1026.
doi:10.1109/TAES.2013.120543

[14] Schaub, H., and Junkins, J. L., *Analytical Mechanics of Space Systems*, AIAA Education Series, AIAA, Reston, VA, 2014, Chaps. 4, 8.

[15] Allard, C., Schaub, H., and Piggott, S., "General Hinged Solar Panel Dynamics Approximating First-Order Spacecraft Flexing," *AAS Guidance and Control Conference*, AAS Paper 16-156, Breckenridge, CO, Feb. 2016.

[16] Allard, C., Diaz-Ramos, M. F., and Schaub, H., "Spacecraft Dynamics Integrating Hinged Solar Panels and Lumped-Mass Fuel Slosh Model," *AIAA/AAS Astrodynamics Specialist Conference*, AIAA Paper 2016-5684, 2016.
doi:10.2514/6.2016-5684

[17] Kane, T. R., and Levinson, D. A., *Dynamics: Theory and Applications*, McGraw–Hill, New York, 1985, Chaps. 1–2.

[18] Shuster, M. D., "A Survey of Attitude Representations," *Journal of the Astronautical Sciences*, Vol. 41, No. 4, 1993, pp. 439–517.